



Alpine Holocene Tree-Ring Dataset: Age-related trends in the stable isotopes of cellulose show species-specific patterns.

Tito Arosio^{1,2}, Malin M. Zieher^{1,2,5}, Kurt Nicolussi³, Christian Schlüchter^{2,4}, Markus Leuenberger^{1,2}

¹Climate and Environmental Physics, Physics Institute, University of Bern, 3012 Bern, Switzerland

²Oeschger Centre for Climate Change Research, University of Bern, 3012 Bern, Switzerland

³Department of Geography, Universität Innsbruck, 6020 Innsbruck, Austria

⁴Institute of Geological Sciences, University of Bern, 3012 Bern, Switzerland

⁵Swiss Tropical and Public Health Institute, Socinstrasse 57, 4051 Basel, Switzerland

Correspondence to: Tito Arosio (tito.arosio@climate.unibe.ch)

10 **Abstract.** Stable isotopes in tree-ring cellulose are important tools for climatic reconstructions even though their interpretation
could be challenging due to non-climate signals, primarily those related to tree ageing. Previous studies on the presence of
tree-age related trends during juvenile as well as adult growth phases in δD , $\delta^{18}O$ and $\delta^{13}C$ time series yielded variable results
that are not coherent among different plant species. We analysed possible trends in the extracted cellulose of tree-rings of 85
15 larch trees and 119 cembran pine trees, i.e. in samples of one deciduous and one evergreen conifer species collected at the
treeline in the Alps covering nearly the whole Holocene. The age trend analyses of all tree-ring variables were conducted on
the basis of mean curves established by averaging the cambial-age aligned tree series. For cambial ages over 100 years, our
results prove the absence of any age-related effect in the δD , $\delta^{18}O$ and $\delta^{13}C$ time series for both the evergreen as well the
deciduous conifer species, with the only exception of larch δD . However, for lower cambial ages, we found trends that differ
20 for each isotope and species. I.e., mean $\delta^{13}C$ values in larch do not vary with ageing and can be used without detrending,
whereas those in cembran pine show a juvenile effect and the data should be detrended. Mean $\delta^{18}O$ values present two distinct
ageing phases for both species complicating detrending. Similarly, mean δD values in larch change in the first 50 yr whereas
cembran pine between 50-100 yr. Values for these two periods of cambial age for δD and $\delta^{18}O$ should be used with caution
for climatic reconstructions, ideally complemented by additional information regarding mechanisms for these trends.

1 Introduction

25 Stable isotopes in tree-ring cellulose are powerful tools for climatic reconstructions (Kress et al. 2010; Nagavciuc et al. 2019).
An advantage of stable isotope time-series based on tree-rings compared to other isotope time series is the defined dating and
temporal, e.g. annual, resolution. A challenge for the climatic interpretation of many tree ring parameters is the presence of
non-climate signals, primarily those related to tree ageing. Tree-ring width (TRW) and maximum latewood density show
ageing effects, which usually have to be removed with detrending/standardization procedures before using them for climatic
30 reconstruction (Helama 2017). A key question for isotope dendroclimatology is whether isotope ratios of the tree cellulose



also show age trends (McCarroll and Loader 2004), still a controversial issue depending on isotope type and plant species. If tree-age related trends are absent the analysis and reconstruction of long-term climatic evolutions based on tree-ring isotope series would lose a source of potential bias.

For $\delta^{13}\text{C}$, ageing studies were initiated by Freyer et al. (1979) on many tree species, followed by other investigations on, e.g.,
35 pines, oaks and beeches. All documented an increase for $\delta^{13}\text{C}$ values in the juvenile period (Anderson et al. 2005; Duquesnay et al. 1998; Gagen et al. 2008; Li et al. 2005; McCarroll and Pawellek 2001; Monserud and Marshall 2001; Nagavciuc et al. 2019; Raffalli-Delercé et al. 2004; Treydte et al. 2001). A “long term trend” with continuous increase of $\delta^{13}\text{C}$ values during the entire life of *Pinus sylvestris* was also described (Helama et al. 2015). An early juvenile effect in the first 5 yr was reported for oak (Duffy et al. 2017). Fewer works did not detect any juvenile or long-term trend of $\delta^{13}\text{C}$ values in *Pinus sylvestris* and
40 larch (Gagen et al. 2007; Kilroy et al. 2016; Young et al. 2011). Altogether, most studies found a juvenile trend (increase), but of variable lengths.

An initial work on $\delta^{18}\text{O}$ values found a negative juvenile trend of 300 yr in *Juniperus turkestanica* grown at elevations around 3000 m a.s.l. (Treydte et al. 2006). A similar negative juvenile trend of 300 y was reported also in *Pinus uncinata*, (Esper et al. 2010). A positive trend of 30 yr was found for oak (Labuhn et al. 2014) and positive “long term trends” were reported for
45 spruce and beeches (Klesse et al. 2018). In contrast, other studies did not find detectable age trends in larch, oak, *Pinus sylvestris*, *Abies alba*, cembra pine (Daux et al. 2011; Duffy et al. 2017; Duffy et al. 2019; Nagavciuc et al. 2019; Saurer et al. 2000; Young et al. 2011). Thus, the studies on $\delta^{18}\text{O}$ trends are rather controversial, showing negative, positive or no age-related trends. The mentioned studies analyzed trees from different geographical origins, including some from sites near the treeline where trees often grow in open space. Such growth situations may have an effect on age trends, i.e., under open space
50 growth there is no neighbourhood competition and therefore no limitation of growth by adjacent trees (Matsushita et al. 2015). The absence of a canopy effect may modify also the isotope composition stored by the trees, as shown for $\delta^{18}\text{O}$ (Daux et al. 2011; Esper et al. 2010; Gagen et al. 2008; Nagavciuc et al. 2019; Young et al. 2011). Furthermore, open space growing limits effects described previously such as tree dominance-suppression or location/exposition effects (wet – dry; sunny – shady) (Leuenberger, 2007) that may lead to age trends. The tree height also imposes a hydraulic limitation and possibly reduces
55 stomatal conductance that may lead to an increase of the cellulose $\delta^{13}\text{C}$ values with increasing age (Brienen et al., 2017).

Changes of δD values in relation to tree ages have been analyzed only in two studies. One found a positive juvenile trend of 20 yr followed by a flat phase in spruce trees (Lipp et al. 1993) and the other identified a positive long-term trend in oak (Mayr et al. 2003).

Helama et al. (2015) suggested that the availability of a suitable database of tree-ring isotopes would allow to detect age trends
60 and would open possibilities to their elimination in order to improve the recognition of long-term climatic evolution. Five issues were indicated as necessary for such a database: i) that it contains a large sample number, ii) that it has no data from



“pooled” rings, iii) that the samples are well distributed over calendar years with different climate conditions, iv) that the samples come from timberline or treeline sites, where the distance between the trees is large, i.e., limiting the canopy effect, v) that they do not contain “modern” rings that need to be corrected in $\delta^{13}\text{C}$ for the anthropogenic rise of CO_2 concentration
65 in the atmosphere.

Here we investigated the presence of age trends by utilizing a stable-isotope tree-ring database which was established on the base of the Eastern Alpine Conifer Chronology (Nicolussi et al. 2009). The database consists of i) samples of mainly subfossil wood from 201 trees, ii) the isotope samples are not pooled, iii) the isotope time series with up to multi-centennial length are continuously covering the last ca. 9000 years, iv) it utilizes two different species: deciduous larch and evergreen cembran pine,
70 v) the wood material was collected at different treeline sites and vi) it contains only 17 trees with rings that grew after the industrial revolution. In the present work we aim to verify the presence of age trends in δD , $\delta^{18}\text{O}$ and $\delta^{13}\text{C}$ in comparison with those of cellulose content (CC) and TRW. We considered the whole, multi-centennial cambial age range of the trees to identify and quantify the length and extent of the juvenile and the long-term ageing periods.

2 Material and methods

75 2.1 Subfossil wood samples and sampling sites in the Alps

Holocene wood sections were available at the Department of Geography of the University of Innsbruck, where the Eastern Alpine Conifer Chronology (EACC) has been established on the base of calendar-dated tree-ring width series (Nicolussi et al. 2009). We have utilized a large number of these subfossil wood samples that cover nearly the whole Holocene (Nicolussi et al. 2009). They belong to the deciduous larch (*Larix decidua* Mill.) and the evergreen cembran pine (*Pinus cembra* L.) and
80 have been collected at treeline sites for paleo-climatic studies. The sampling sites are located in different parts of the European Alps covering a SW-NE transect with an elevation range of 1,930 to 2,400 m (Fig. 1). The wood material was collected at 29 different sites, 3 of them have only larch, 15 only cembran pine and 11 sites contain both species. The characteristics of the 201 trees are listed in Table 1. Only 17 of them contain tree rings formed after the industrial revolution, i.e. after ca. 1850 AD. Samples of 5-year spanning wood have been prepared and analyzed for stable isotope ratios, as described before (Ziehmer et
85 al. 2018; Arosio et al., 2020).

2.2 Tree-ring width data and cambial age estimation

The tree-ring width of all the samples were measured with a precision of 0.001 mm as described in Nicolussi et al. (2009). Dated tree samples with relatively wide rings were selected to collect enough material for the isotope measurements. In subfossil specimen the number of rings available for analyses often do not cover the whole tree lifespan due to effects of decay
90 processes and therefore the cambial age of the first measured ring was estimated from ring curvature for tree samples without preserved pith (Nicolussi et al. 2009)



2.3 Stable isotope analysis

The procedure of cellulose extraction, determination of the cellulose content (cellulose dry weight / wood dry weight) (Ziehmer et al. 2018) and the triple-isotope analysis were described before (Loader et al. 2015). Briefly, we used conventional Isotope
95 Ratio Mass Spectrometry (Isoprime 100) coupled to a pyrolysis unit (HEKAtech GmbH, Germany), which is similar to the
previously used TC/EA (for technical details see (Leuenberger 2007)). This approach was extended to measurements of non-
exchangeable hydrogen of alpha-cellulose using the on-line equilibration method (Filot et al. 2006; Loader et al. 2015). The
results are reported in per mil (‰) relative to the Vienna Pee Dee Belemnite (VPDB) for carbon and to Vienna Standard Mean
Ocean Water (VSMOW) for hydrogen and oxygen (Coplen 1994). The precision of the measurement is $\pm 3.0\text{‰}$ for hydrogen,
100 $\pm 0.3\text{‰}$ for oxygen and $\pm 0.15\text{‰}$ for carbon (Loader et al. 2015).

2.4 Carbon isotope correction

The burning of fossil fuels and land-use changes of the Industrial Period from about 1850 onwards caused a continuous increase
of atmospheric carbon dioxide (CO₂) depleted in $\delta^{13}\text{C}$ (Leuenberger 2007) known as Suess Effect (Suess 1955). This change
is reflected in the carbohydrates of the plants, therefore a correction has to be applied to the isotopic series of tree rings. For
105 all the $\delta^{13}\text{C}$ values after the 1000 AD we applied the correction factor described in Leuenberger (2007).

2.5 Age trend analysis

Each tree series was aligned on the cambial age and larch and cembran pine samples were analyzed independently. The values
of the three isotope ratios were analyzed as raw, normalized and z-scored data. The normalization consisted in subtracting the
mean of the time series of a tree from each raw value of this series. For the analysis of the age-related trends, the isotope series
110 of these three data groups were averaged to mean series for both investigated species under consideration of cambial age of
the tree time series. We limited the analysis of these isotope mean series to the cambial age period where the replication number
is ≥ 10 (Klesse et al. 2018; Young et al. 2011). We plotted the normalized data of the isotope values versus the cambial age
of the trees. Then we applied a linear interpolation in the different parts of the curves to quantify the trend. The division of the
curves is different for each isotope, showcasing their different behaviours. The same procedure was applied to TRW and CC
115 series, but for TRW we used the raw in place of the normalized data. To verify the presence of trends we applied a linear fit
and compared it with those of the isotopes.

3 Results

Our aim was to interrogate the stable isotopes of the EACC database for age effects using the well-known age-trends in TRW
120 as comparison. The plot of the cambial age versus calendar age (Fig. 2A) shows that the database includes isotope time series



covering age ranges from 15 to 610 years, with only few of them starting from the pith. The cambial ages of the trees are rather uniformly distributed over the entire Holocene, thus avoiding a potential bias in the analysis of age-trend. Figure 2A also shows that the time series of the two species, larch (red) and cembran pine (green) are similarly distributed over the Holocene. The sample replication number per cambial age of the trees is shown in figure 2B, with the horizontal line indicating the
125 threshold ≥ 10 , that ranged from 1 to 460yr for cembran pine and from 10 to 480yr for larch. We considered this replication threshold important in this study,

The isotope series of the individual larch trees have a mean length of 273 yr (with a minimum and maximum length of 25 and 550 yr, respectively), the mean of their initial measure is 75 yr and the mean final cambial age is 348 yr. The individual cembran pine time series have a mean length of 257 yr (with a minimum and maximum length of 15 and 610 yr, respectively),
130 the mean of their initial data point is 67 yr and the mean final cambial age is 324 yr. Table 1 describes the samples we analyzed and shows that they cover the period 8930 b2k to 2010 A.D., with a maximum cambial age of 725 yr.

The means of raw data of each isotope of larch and cembran pine were plotted versus cambial age (Fig 3B, 4B, 5B). The absolute mean values differ probably because of different geographical origin of the trees or species-specific signature (Arosio et al., 2020), therefore we analyzed also the trend with the normalized data. The geographical effect may influence not only
135 the mean but also the variance of each series, thus altering the age trend. To verify it, we used the z-scored data by dividing the normalized values by the standard deviation for each tree. No consistent difference was found between the normalized and z-score data (supplemental, fig. S1), indicating that the variance of the isotope series was not significantly influenced by geographical factors.

We found that all average isotope series show trend changes only in the first 100 yr of cambial age in agreement with previous
140 reports (Esper, 2015) except δD of larch. Therefore, we analyzed the average series, before and after 100 yr, separately. The trends of the average series with sample replication above or equal to 10 for all subperiods were studied by linear correlations, as in Young et al. (2011).

3.1 $\delta^{13}\text{-Carbon}$

Means of the standardized $\delta^{13}\text{C}$ data of all samples from 1 to about 500 cambial yr of both species are shown in figure 3A.
145 Data points with a replication of ≥ 10 are considered, as shown in the replication plot of figure 2A. The plots of the raw and of the normalized data are shown in figure 3B. The mean raw values of cembran pine (cyan) are more depleted than the ones of larch (red) (Fig. 3B). After normalization the mean values of the two species overlap only partially, since in the juvenile phase of the two species show different trends (fig 3B). Mean values for larch are stable, while the cembran pine documents a strong positive trend in the first 100 yr ($0.7\text{‰}/100\text{ yr}$) followed by a stabilization (Fig. 3C).



150 3.2 $\delta^{18}\text{O}$ -Oxygen

The same approach was used to study the variation of $\delta^{18}\text{O}$ of all samples (Fig. 4A) with their mean values in light green. Raw and normalized data are shown in figure 4B. The larch raw data are evidently more $\delta^{18}\text{O}$ enriched than the cembran pine ones, and the normalization strongly reduces the difference between the two species and the two time series are almost overlapping (fig 4B, right). In Figure 4C only the normalized averages series of the two species are plotted. Both of them show a peak in
155 the first 100 yr followed by a phase without major age trend. Linear regression was applied to separate an initial phase of 50 yr with increasing values, followed by a sharp decrease until 100 yr and then a stabilization. The initial increasing phase in the larch was less steep than that in cembran pine, and for the rest the patterns are similar.

3.3 δ -Deuterium

Means of the standardized δD data of all samples from 1 to about 500 cambial yr of the two species are shown in figure 5A.
160 Means of δD raw values clearly indicate that larch is more depleted than cembran pine (fig. 5B, left) as shown before (Arosio et al. 2020). After normalization the two plots partially overlap (fig 5B, right). Figure 5C shows the means of the two species, the pattern of which are rather different. Larch shows a steep initial decrease in the first 50 yr, after a short steep increase within 10 years the values follows a minor increase through all the time, the cembran pine documents an initial slight decrease in the first 50 yr, followed by a steep positive trend of 50 yr and a flat line from 100 yr on (Fig. 5E).

165 3.4 TRW

The same analysis has also been applied to the non-detrended tree-ring width values, with the difference that in fig 6A the raw data are used. Figure 6A shows all the raw values and the mean value in light green. The plots of the raw and normalized data, expressed in cm, show a similar trend (Fig. 6B). Means with a replication ≥ 10 (Fig 6B and C) show a maximum at around 30 yr, in agreement with previous reports (Bräker 1981), after which the values of both species steadily decrease in two slope
170 sections until 300 yr, thereafter becoming flat (Bräker 1981). For similarity with the isotope analyses, we applied linear regression to the data, instead of the more common exponential regression.

3.5 Cellulose Content

The same analysis has also been applied to data of the cellulose content. Figure 7A shows all raw values and the mean values in light green. The plots of the raw and normalized data, expressed in percent, show a similar trend (Fig. 7B). Means with a
175 replication ≥ 10 (Fig 7B and C) present a remarkable increase in the first 50 yr in both species, from a cambial age of 51 yr to the end the larch presents a decreasing trend, while the cembran pine shows no trend.



4 Discussion

180 A characteristic of our present work is that the wood samples represent two conifer species, consisting of 201 trees that were
collected at 29 different sites at high elevations in the Alps. They were exposed to different environmental conditions such as,
e.g., elevation, aspect, slope steepness and water availability. Therefore, we normalized all records by subtracting by the mean
of the tree from the raw values (Daux et al. 2011). A different approach was used by Helama et al. (2015) who used the raw
data to analyze samples from only three different sites. Here we present analysis of a much more extended database, in time
and space, which certainly represents the natural variability realistically. However, there are still issues that requires
185 consideration, in particular the sample replication. Our database does not have a constant sample replication throughout the
cambial age of the trees. It is low at the beginning and increases in the first 50 yr, and decreases sharply after 450 yr. This may
have some effect on the study of the age trends.

As introduced in the results section, we have divided tree ageing in a juvenile period that we deliberately terminated at 100 yr,
190 and the long-term period that lasted until 450 yr. A major conclusion of this study is that the values of δD , $\delta^{18}\text{O}$ and $\delta^{13}\text{C}$ in
long term period from 100 yr to 450 yr did not change significantly, except δD in larch. This is in agreement with previous
 $\delta^{13}\text{C}$ studies on evergreen conifers (Esper et al. 2015; Gagen et al. 2007; Gagen et al. 2008; Klesse et al. 2018; Nagavciuc
et al. 2019; Saurer et al. 2004; Young et al. 2011) and with the $\delta^{18}\text{O}$ previous studies on larch (Daux et al. 2011; Kilroy et al.
2016; Nagavciuc et al. 2019). This implies that no detrending is necessary of tree isotope data for climate analysis with cambial
195 age in that range, with the exception of δD in larch where a non-significantly trend is present.

More complex are the data of the juvenile period, during which the trend behavior differs among the different isotopes and
species. In the juvenile phase we found evidence for a positive trend of $\delta^{13}\text{C}$ in evergreen cembran pine but not in deciduous
larch. These data are in good agreement with studies on evergreen conifers (*Picea abies*, *Pinus sylvestris*, *Pinus uncinata*) that
200 all found an initial positive trend lasting up to 50 yr (Gagen et al. 2007; Gagen et al. 2008), or 100 yr (Klesse et al. 2018) or
200 yr (Esper et al. 2015). Moreover, two previous studies on larch did not report any evident trend for $\delta^{13}\text{C}$ in the juvenile
period (Daux et al. 2011; Kilroy et al. 2016b). We can conclude that there is a general agreement that deciduous larch and
evergreen conifers behave differently in the juvenile period in respect to $\delta^{13}\text{C}$ of the cellulose. Further work is needed to
understand the reason of this difference.

205 The behavior of $\delta^{18}\text{O}$ values in the initial period is rather complex, with a maximum around 50 yr and a decrease up to 100 yr
in both species. This is in good agreement with a previous work, that showed, that in *Pinus uncinata* grown at the tree-line
have maximal $\delta^{18}\text{O}$ values around 20-50 yr followed by a negative trend (Esper et al. 2010) and another study on beech and
spruce that found a positive juvenile trend the persisted beyond 50 years of age (Klesse et al. 2018). Altogether, our data show
210 that $\delta^{18}\text{O}$ of cellulose of larch and cembran pine has ageing trends that are similar to those of other tree species, with up and



down trends in the first 100 yr and an intermediate maximum at around 50 yr. The significance of these trends remain to be further studied. However, considering the time and space of our database covers, this result seems to be widespread and temporally robust.

215 Our results on δD demonstrate different patterns for larch and cembran pine in the juvenile period, similarly to $\delta^{13}C$. The evergreen cembran pine displays an initial flat phase of 25 yr, then an increase of 4‰ till 100 yr. This is in partial agreement with a previous work that showed an increase of δD values in the juvenile period, but this lasted only 20 yr (Lipp et al. 1993). Another work measured δD by nitration of the cellulose to remove non-exchangeable hydrogens (Leavitt 2010), but this is certainly not the reason for this difference, as demonstrated by Filot et al. (2006). The difference can be attributed to the
220 different growth environments of the trees, one at an elevation of 330 m near Bad Windsheim (Germany) and the other at a mean altitude of 2100 m, at tree-line sites in the Alps, where tree growth is known to be much slower with prolonged juvenile phase (Körner 2003; Ott 1978). The only other work that analyzed the evolution of δD in cellulose during ageing reported a constant increase of δD values in the first 175 years in oak (Mayr et al. 2003). In our work the deciduous larch showed a different pattern with a strong decrease of δD values in the first 50 yr, followed by a feeble increase smaller than the analytical
225 precision. We have not found other studies that dealt with δD in larch

The effect of TRW has been studied for long and is well documented (e.g., Helama et al., 2017). After a very short (< 20 yr) period of increasing TRW values, they consistently decrease, yet with different rates. From 20 to 100 yr the decrease is rather steep thereafter changing to moderate rates. At around 300 yr of cambial age they are flattening out in both species.
230 Understanding the absolute growth rate change is rather complex as discussed for instance in Matsushita et al. (2015). Dependencies of the age-size, growth-size and growth-age relationships are crucial. The fact that our database consists of trees from tree-line sites allows us to state that our derived trends are independent from the so-called crowding effect (influence of neighboring trees). Therefore, it represents mainly the individual variability and the age-size influence on the growth rate. We did not find any dependence of the trends in the different selected time frames within the past 9,000 yr, the behavior we
235 observed should represent the general dependence of the age-size influence.

The decay of wood does not influence the carbon and oxygen stable isotope values of the cellulose (Nagavciuc et al. 2018), but that it can impact CC, since the cellulose is decomposed faster than lignin. Yet, it has been shown that CC has the potential to be used as a climate proxy (Ziehmer et al., 2018). In the analysis of tree-age related trends we have to consider that the
240 decay of a trunk is not equal for all parts, and that hardwood in contrast to sapwood presents a decay resistance, which also varies from species to species (Kéérik, 1974). Both investigated species show a similar positive trend in approximately the first 50 yr of cambial age followed by a slight negative trend for larch or no overall trend for cembran pine. This suggests, with reference to our data, that there are probably no (cembran pine) or possibly only minor (larch) influences due to effects of wood decay. This suggests that the CC variation in the first 50 yr is not due to wood decay, but rather a tree-ageing effect.



245

5 Conclusions

The present work confirms the absence of an ageing effect for all three stable isotopes after 100 yr of cambial age in the two conifer species, suggesting that the values older than 100 yr of cambial age can be considered for climate analyses without detrending. The exception is larch that shows a minor increase of δD mean values, smaller than the analytical precision. Before 100 yr the trends differ for each isotope and species, and only the larch $\delta^{13}C$ values can be used without detrending, since they do not vary with ageing. In both species, the $\delta^{18}O$ values present two phases, making the detrending rather challenging. It is similar for δD values in larch that change in the first 50 yr, whereas in cembran pine between 50-100 yr. Again detrending is demanding and should ideally be complemented by additional information regarding an explanation of this behavior. Tree ring cellulose contents show a significant trend for the first 50 years only, in contrast tree ring width curves flattening only after 300 year. Here the application of a regional curve standardization (RCS) is valuable. In summary, for climate reconstructions isotope data older than 100 cambial yr can be use directly, data of the first 100 yr should be used with caution. Therefore, data can be used only after detrending or when compared with data from other age classes covering the same time.

260 Acknowledgments.

We are grateful to Peter Nyfeler for the precious assistance during measurements of the stable isotopes, to Andrea Thurner and Andreas Österreicher for the preparation of the isotope samples from Alpine sites and the civil service collaborators: Lars Herrmann, Giacomo Ruggia, Jonathan Lamprecht, Yannick Rohrer, Rafael Zuber. The project is funded by the Swiss National Science Foundation (SNF 200021L_144255, SNF 200020_172550) as well as by the Austrian Science Fund (FWF, grant I-1183-N19) and is supported by the Oeschger Center for Climate Change Research, University of Bern, Bern, Switzerland (OCCR).\$

*Competing interests.*The authors declare that they have no conflict of interest

Author contribution statement

270 TA and MZ performed the stable isotope analyses, TA drafted the first version of the manuscript. KN collected the samples and made the crossdating. ML contributed to the evaluation of the results. ML, KN, CS conceived of the presented idea. All authors provided comments to improve the manuscript.



References

- Anderson, W.T., Sternberg L., Pinzon M., Gann T. -Troxler. Childers, D.L and Duever M.: Carbon isotopic composition of
275 cypress trees from South Florida and changing hydrologic conditions. *Dendrochronologia*. 23:1-10.
<https://doi.org/10.1016/j.dendro.2005.07.006>, 2005
- Arosio, T., Ziehmer M. M., Nicolussi K., Schlüchter C., Leuenberger M.: Larch cellulose is significantly depleted in deuterium
isotopes with respect to evergreen conifers – Submitted, 2020
- Bräker, O.-U. der alterstrend bei jahringdichten und jahringbreiten von nadelhoebyzern und sein ausgleich, 1981
- 280 Brienen, R.J.W., Gloor, E., Clerici, S., Newton, R., Arppe, L., Boom, A., Bottrell, S., Callaghan, M., Heaton, T., Helama, S.
and Helle, G.: Tree height strongly affects estimates of water-use efficiency responses to climate and CO₂ using
isotopes. *Nature Communications*, 8(1), pp.1-10. <https://doi.org/10.1038/s41467-017-00225-z>, 2017
- Coplen, T.B.. Reporting of stable hydrogen, carbon, and oxygen isotopic abundances (technical report). *Pure and Applied
Chemistry*, 66(2), pp.273-276. <https://doi.org/10.1351/pac199466020273>, 1994
- 285 Daux, V., Edouard J., Masson-Delmotte V., Stievenard M., Hoffmann G., Pierre M., Mestre O., Danis P. and Guibal F... Can
climate variations be inferred from tree-ring parameters and stable isotopes from *Larix decidua*? Juvenile effects,
budmoth outbreaks, and divergence issue. *Earth Planetary Science Letters*. 309:221-233.
<https://doi.org/10.1016/j.epsl.2011.07.003>, 2011
- Duffy, J.E., McCarroll D., Barnes A., Ramsey C.B., Davies D., Loader N.J., Miles D. and Young G.H.. Short-lived juvenile
290 effects observed in stable carbon and oxygen isotopes of UK oak trees and historic building timbers. *Chemical
Geology*. 472:1-7. <https://doi.org/10.1016/j.chemgeo.2017.09.007>, 2017
- Duffy, J.E., McCarroll D., Loader N.J., Young G.H., Davies D., Miles D. and Bronk Ramsey C. Absence of age-related trends
in stable oxygen isotope ratios from oak tree rings. *Global Biogeochemical Cycles*. 33:841-848.
<https://doi.org/10.1029/2019GB006195>, 2019
- 295 Duquesnay, A., Breda N., Stievenard M. and Dupouey J.. Changes of tree-ring $\delta^{13}\text{C}$ and water-use efficiency of beech (*Fagus
sylvatica* L.) in north-eastern France during the past century. *Plant, Cell Environment*. 21:565-572.
<https://doi.org/10.1046/j.1365-3040.1998.00304.x>, 1998
- Esper, J., Frank, D.C., Battipaglia, G., Büntgen, U., Holert, C., Treydte, K., Siegwolf, R. and Saurer, M. Low-frequency noise
in $\delta^{13}\text{C}$ and $\delta^{18}\text{O}$ tree ring data: A case study of *Pinus uncinata* in the Spanish Pyrenees. *Global Biogeochemical
300 Cycles*, 24(4). <https://doi.org/10.1029/2010GB003772>, 2010
- Esper, J., Konter, O., Krusic, P.J., Saurer, M., Holzkämper, S. and Büntgen, U., Long-term summer temperature variations in
the Pyrenees from detrended stable carbon isotopes. *Geochronometria*, 53:59, 42(1). DOI 10.1515/geochr-2015-0006,
2015



- Esper, J., Klippel, L., Krusic, P.J., Konter, O., Raible, C.C., Xoplaki, E., Luterbacher, J. and Büntgen, U. Eastern Mediterranean
305 summer temperatures since 730 CE from Mt. Smolikas tree-ring densities. *Climate Dynamics*, 54(3), 1367-1382,
<https://doi.org/10.1007/s00382-019-05063-x>, 2020
- Filot, M.S., Leuenberger M., Pazdur A. and Boettger T. Rapid online equilibration method to determine the D/H ratios of non-
exchangeable hydrogen in cellulose. *Rapid Communications in Mass Spectrometry: An International Journal Devoted
to the Rapid Dissemination of Up-to-the-Minute Research in Mass Spectrometry*. 20:3337-3344.
310 <https://doi.org/10.1002/rcm.2743>, 2006
- Freyer, H. On the ^{13}C record in tree rings. Part I. ^{13}C variations in northern hemispheric trees during the last 150 years. *J
Tellus*. 31:124-137. <https://doi.org/10.3402/tellusa.v31i2.10417>, 1979
- Gagen, M., McCarroll D., Loader N.J., Robertson I., Jalkanen R. and Anchukaitis K. Exorcising the segment length curse':
summer temperature reconstruction since AD 1640 using non-detrended stable carbon isotope ratios from pine trees
315 in northern Finland. *The Holocene*. 17:435-446, <https://doi.org/10.1177/0959683607077012>, 2007
- Gagen, M., McCarroll D., Robertson I., Loader N.J. and Jalkanen R.. Do tree ring $\delta^{13}\text{C}$ series from *Pinus sylvestris* in northern
Fennoscandia contain long-term non-climatic trends? *Chemical Geology*. 252:42-51,
<https://doi.org/10.1016/j.chemgeo.2008.01.013>, 2008
- Helama, S., Melvin, T. M., and Briffa, K. R.: Regional curve standardization: State of the art, *Holocene*, 27, 172–177,
320 <https://doi.org/10.1177/0959683616652709>, 2017
- Helama, S., Arppe L., Timonen M., Mielikäinen K. and Oinonen M.. Age-related trends in subfossil tree-ring $\delta^{13}\text{C}$ data.
Chemical Geology. 416:28-35, <https://doi.org/10.1016/j.chemgeo.2015.10.019>, 2015
- Kéérik, A.A. Decomposition of wood. *Biology of plant litter decomposition*, 1, p.129, 1974
- Kilroy, E., McCarroll D., Young G.H., Loader N.J. and Bale R.J. Absence of juvenile effects confirmed in stable carbon and
325 oxygen isotopes of European larch trees. *Acta Silvae et Ligni*:27-33, DOI 10.20315/ASetL.111.3, 2016
- Klesse, S., Weigt R., Treydte K., Saurer M., Schmid L., Siegwolf R.T. and Frank D.C. Oxygen isotopes in tree rings are less
sensitive to changes in tree size and relative canopy position than carbon isotopes. *Plant, cell environment*. 41:2899-
2914, <https://doi.org/10.1111/pce.13424>, 2018
- Körner, C. Alpine plant life: functional plant ecology of high mountain ecosystems; with 47 tables. ed. *Springer Science &
330 Business Media*. Berlin - Heidelberg, DE, 2003
- Kress, A., Saurer, M., Siegwolf, R.T., Frank, D.C., Esper, J. and Bugmann, H. A 350 year drought reconstruction from Alpine
tree ring stable isotopes. *Global Biogeochemical Cycles*, 24(2), <https://doi.org/10.1029/2009GB003613>, 2010
- Labuhn, I., Daux V., Pierre M., Stievenard M., Girardclos O., Féron A., Genty D., Masson-Delmotte V. and Mestre O. Tree
age, site and climate controls on tree ring cellulose $\delta^{18}\text{O}$: A case study on oak trees from south-western France.
335 *Dendrochronologia*. 32:78-89, <https://doi.org/10.1016/j.dendro.2013.11.001>, 2014
- Leavitt, S.W. Tree-ring C–H–O isotope variability and sampling. *Science of the Total Environment*. 408:5244-5253, 2010



- Leuenberger, M. To what extent can ice core data contribute to the understanding of plant ecological developments of the past?
Terrestrial ecology. 1:211-233, <https://doi.org/10.1016/j.scitotenv.2010.07.057>, 2007
- Li, Z.-H., Leavitt S.W., Mora C.I. and Liu R.-M. Influence of earlywood–latewood size and isotope differences on long-term
340 tree-ring $\delta^{13}\text{C}$ trends. *Chemical geology*. 216:191-201, <https://doi.org/10.1016/j.chemgeo.2004.11.007>, 2005
- Lipp, J., Trimborn, P., Graff, W. and Becker, B., Climatic significance of D/H ratios in the cellulose of late wood in tree rings
from spruce (*Picea abies* L.). In *Isotope techniques in the study of past and current environmental changes in the
hydrosphere and the atmosphere*, 1993
- Loader, N., Street-Perrott F., Daley T., Hughes P., Kimak A., Levanič T., Mallon G., Mauquoy D., Robertson I. and Roland T.
345 Simultaneous Determination of Stable Carbon, Oxygen, and Hydrogen Isotopes in Cellulose. *Analytical chemistry*.
87:376-380, <https://doi.org/10.1021/ac502557x>, 2015
- Matsushita, M., Takata, K., Hitsuma, G., Yagihashi, T., Noguchi, M., Shibata, M. and Masaki, T. A novel growth model
evaluating age–size effect on long-term trends in tree growth. *Functional Ecology*, 29(10), pp.1250-1259,
<https://doi.org/10.1111/1365-2435.12416>, 2015
- 350 Mayr, C., Frenzel B., Friedrich M., Spurk M., Stichler W. and Trimborn P.. Stable carbon-and hydrogen-isotope ratios of
subfossil oaks in southern Germany: methodology and application to a composite record for the Holocene. *The
Holocene*. 13:393-402, <https://doi.org/10.1191/0959683603hl632rp>, 2003
- McCarroll, D. and Loader N.J.. Stable isotopes in tree rings. *Quaternary Science Reviews*. 23:771-801,
<https://doi.org/10.1016/j.quascirev.2003.06.017>, 2004
- 355 McCarroll, D. and Pawellek F.. Stable carbon isotope ratios of *Pinus sylvestris* from northern Finland and the potential for
extracting a climate signal from long Fennoscandian chronologies. *The Holocene*. 11:517-526,
<https://doi.org/10.1191/095968301680223477>, 2001
- Monserud, R.A. and Marshall J.D.. Time-series analysis of $\delta^{13}\text{C}$ from tree rings. I. Time trends and autocorrelation. *Tree
physiology*. 21:1087-1102, <https://doi.org/10.1093/treephys/21.15.1087>, 2001
- 360 Nagavciuc, V., Kern, Z., Perșoiu, A., Keșjár, D. and Popa, I. Aerial decay influence on the stable oxygen and carbon isotope
ratios in tree ring cellulose. *Dendrochronologia*, 49, pp.110-117, <https://doi.org/10.1016/j.dendro.2018.03.007>. 2018
- Nagavciuc, V., Ionita M., Perșoiu A., Popa I., Loader N.J. and McCarroll D.. Stable oxygen isotopes in Romanian oak tree
rings record summer droughts and associated large-scale circulation patterns over Europe. *Climate Dynamics*.
52:6557-6568, <https://doi.org/10.1007/s00382-018-4530-7>, 2019
- 365 Nagavciuc, V., Kern, Z., Ionita, M., Hartl, C., Konter, O., Esper, J. and Popa, I., Climate signals in carbon and oxygen isotope
ratios of *Pinus cembra* tree-ring cellulose from the Călimani Mountains, Romania. *International Journal of
Climatology*, 40(5), pp.2539-2556, <https://doi.org/10.1002/joc.6349>, 2020
- Nicolussi, K., Kaufmann M., Melvin T.M., Van Der Plicht J., Schießling P. and Thurner A. A 9111 year long conifer tree-ring
chronology for the European Alps: a base for environmental and climatic investigations. *The Holocene*. 19:909-920,
370 <https://doi.org/10.1177/0959683609336565>, 2009



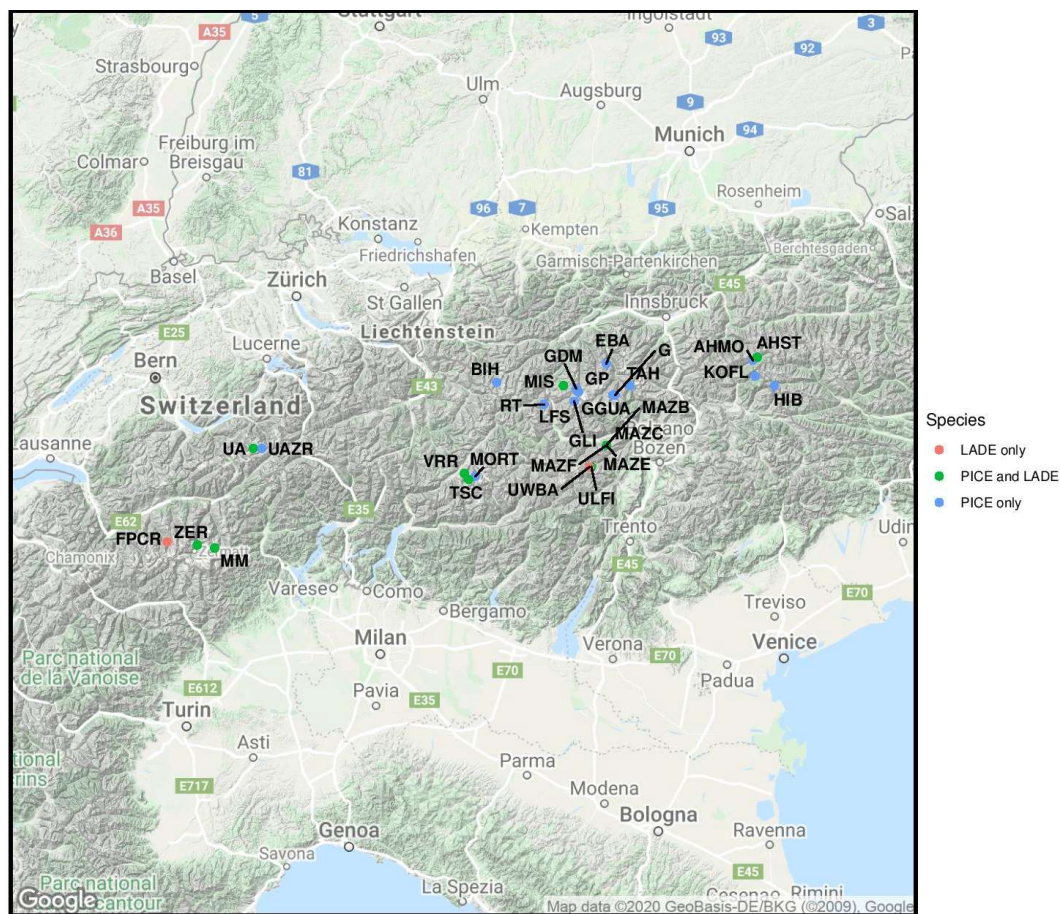
- Ott, E., Über die Abhängigkeit des Radialzuwachses und der Oberhohen bei Fichte und Larche von der Meereshöhe und Exposition im Lotschental. *J For Suisse*. 169:193, 1978
- Raffalli-Delercq, G., Masson-Delmotte V., Dupouey J., Stievenard M., Breda N. and Moisselin J. Reconstruction of summer droughts using tree-ring cellulose isotopes: a calibration study with living oaks from Brittany (western France). *Tellus B: Chemical Physical Meteorology*. 56:160-174, <https://doi.org/10.3402/tellusb.v56i2.16405>, 2004
- 375 Reinig, F., Nievergelt D., Esper J., Friedrich M., Helle G., Hellmann L., Kromer B., Morganti S., Pauly M. and Sookdeo A... New tree-ring evidence for the Late Glacial period from the northern pre-Alps in eastern Switzerland. *Quaternary Science Reviews*. 186:215-224, <https://doi.org/10.1016/j.quascirev.2018.02.019>, 2018
- Saurer, M., Cherubini P. and Siegwolf R. Oxygen isotopes in tree rings of *Abies alba*: The climatic significance of interdecadal variations. *Journal of Geophysical Research: Atmospheres*. 105:12461-12470, <https://doi.org/10.1029/2000JD900160>, 2000
- 380 Saurer, M., Siegwolf R.T. and Schweingruber F.H.. Carbon isotope discrimination indicates improving water-use efficiency of trees in northern Eurasia over the last 100 years. *Global Change Biology*. 10:2109-2120, <https://doi.org/10.1111/j.1365-2486.2004.00869.x>, 2004
- 385 Suess, H.E.. Radiocarbon concentration in modern wood. *Science*. 122:415-417, 1955
- Treydte, K., Schleser G.H., Schweingruber F.H. and Winiger M. The climatic significance of $\delta^{13}C$ in subalpine spruces (Lötschental, Swiss Alps) a case study with respect to altitude, exposure and soil moisture. *Tellus* 53:593-611, <https://doi.org/10.1034/j.1600-0889.2001.530505.x>, 2001
- Treydte, K.S., Schleser G.H., Helle G., Frank D.C., Winiger M., Haug G.H. and Esper J.. The twentieth century was the wettest period in northern Pakistan over the past millennium. *Nature Climate Change*. 440:1179, <https://doi.org/10.1038/nature04743>, 2006
- 390 Young, G.H., Demmler J.C., Gunnarson B.E., Kirchhefer A.J., Loader N.J. and McCarroll D.. Age trends in tree ring growth and isotopic archives: A case study of *Pinus sylvestris* L. from northwestern Norway. *Global Biogeochemical Cycles*. 25:GB2020, <https://doi.org/10.1029/2010GB003913>, 2011
- 395 Ziehmer M.M., Nicolussi K., Schlüchter C. and Leuenberger M.. Preliminary evaluation of the potential of tree-ring cellulose content as a novel supplementary proxy in dendroclimatology. *Biogeosciences*. 15:1047-1064, <https://doi.org/10.5194/bg-15-1047-2018>, 2018



400

SITE	SPECIES	N TREES	MEAN LENGTH (YR)	COORDINATES	ASPECT	ELEVATION (m)
AHMO	PICE	16	178	47°03'E/12°08'N	SE	1995
AHST	LADE	2	125	47°05'E/12°11'N	S	2080
	PICE	2	93			
BIH	PICE	1	190	46°91'E/10°10'N	N	2175
EBA	PICE	11	196	47°01'E/10°95'N	NE	2115
FPCR	LADE	4	208	46°06'E/7°55'N	WSW	1965
G	PICE	3	215	46°85'E/11°01'N	NW	2060
GDM	PICE	15	197	46°88'E/10°71'N	E	2295
GGUA	PICE	3	160	46°85'E/11°N	W	2175
GLI	PICE	6	164	46°81'E/10°7'N	NE	2147.5
GP	PICE	5	86	46°86'E/10°73'N	W	2167.5
HIB	PICE	1	180	46°9' E/12°25'N	E	2140
KOFL	PICE	1	130	46°95'E/12°1'N	S	2177.5
LFS	PICE	2	148	46°81' E/10°7'N	NW	2335
MAZB	LADE	6	162	46°58'E/10°95'N	N	2125
	PICE	2	198			
MAZC	LADE	4	160	46°58'E/10°95'N	N	2120
MAZE	LADE	5	188	46°58'E/10°95'N	N	2125
	PICE	8	124			
MAZF	LADE	2	250	46°58'E/10°95'N	N	2105
	PICE	1	155			
MIS	LADE	1	125	46°9'E/10°61'N	N	2252.5
	PICE	1	275			
MM	LADE	6	247	46°03'E/7°916'N	NNE	1995
	PICE	7	260			
MORT	PICE	3	253	46°41'E/9°933'N	W	2045
RT	PICE	2	258	46°8'E/10°46'N	SE	2400
TAH	PICE	3	195	46°9'E/11°13'N	S	2117.5
TSC	LADE	7	206	46°4'E/9°88'N	NW	2162.5
	PICE	7	256			
UA	LADE	17	168	46°56'E/8°21'N	E	1950
	PICE	2	205			
UAZR	PICE	4	173	46°56'E/8°28'N	SSE	1977
ULFI	LADE	24	243	46°46'E/10°83'N	N	2110
	PICE	4	208			
UWBA	LADE	2	200	46°46'E/10°81'N	NE	2330
VRR	LADE	4	219	46°43'E/9°85'N	E	2158.5
	PICE	5	209			
ZER	LADE	1	295	46°05'E/7°78'N	N	2315
	PICE	1	110			

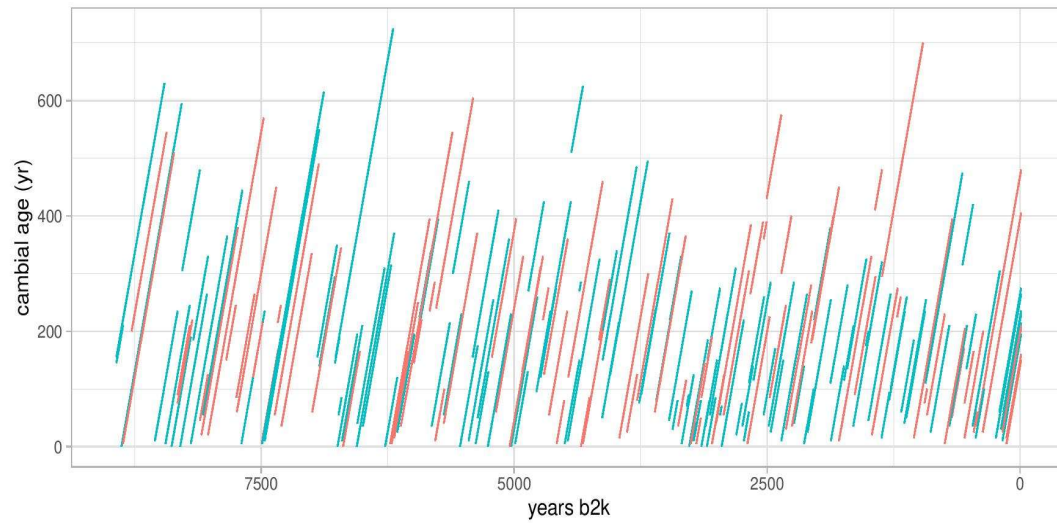
425 **Table 1.** Characteristics of the sampling site and of the trees: 11 sites contain both larch and cembran pine samples, 2 sites contain only larch (LADE) specimens and the remaining sites only cembran pine (PICE)



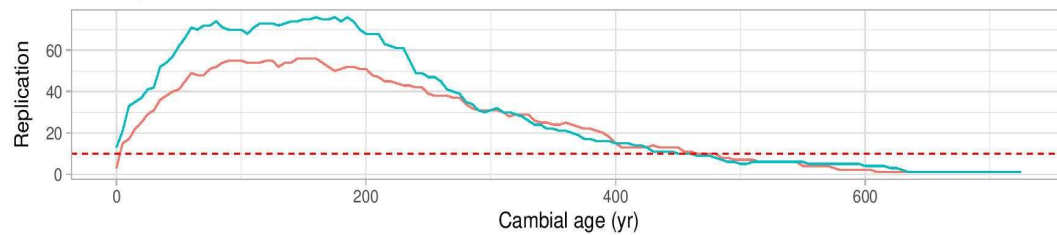
430 **Figure 1.** Map of the location of the 29 sampling sites (© Google Maps 2020): They are situated in the Swiss, the Austrian and the Italian Alps. Information to each site is given in table 1.



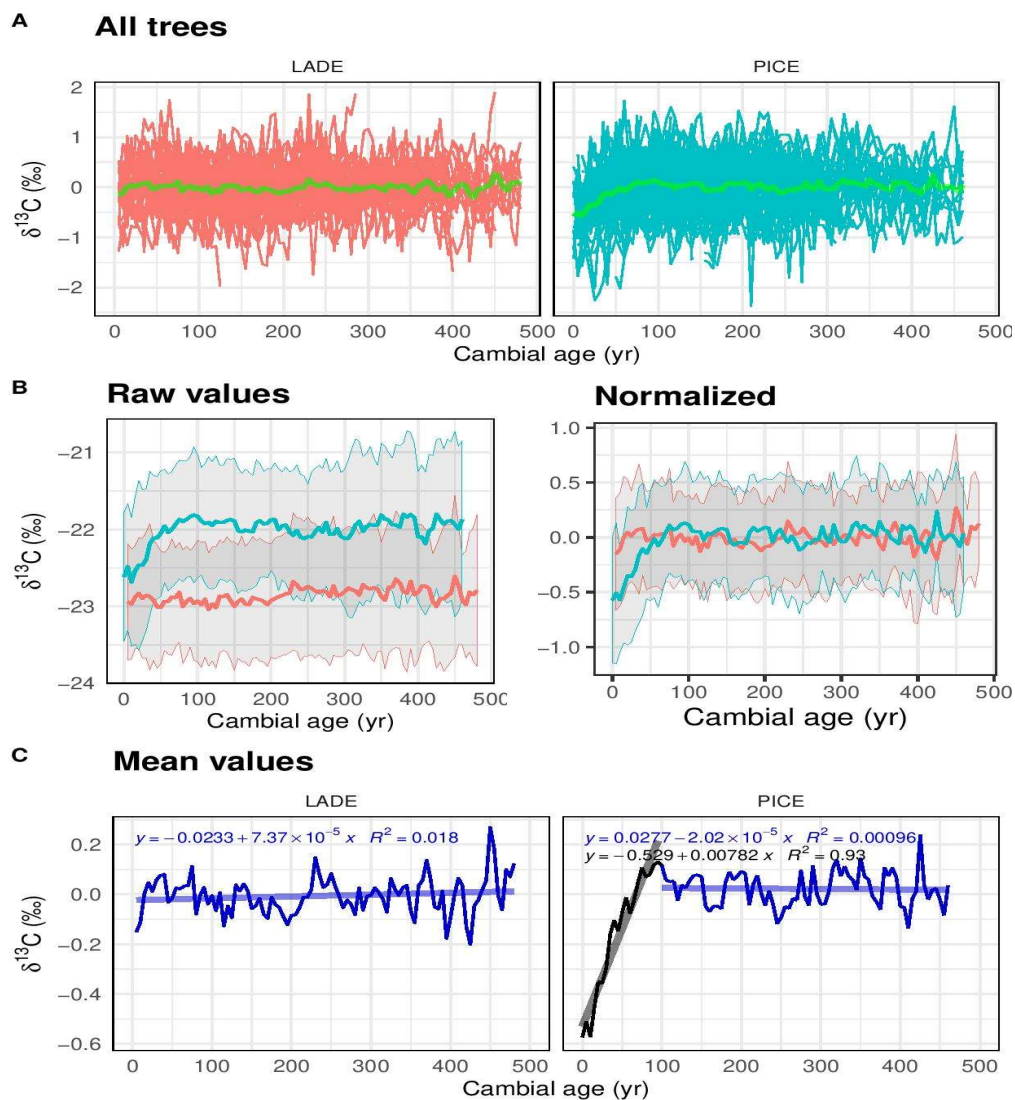
A cambial age vs time



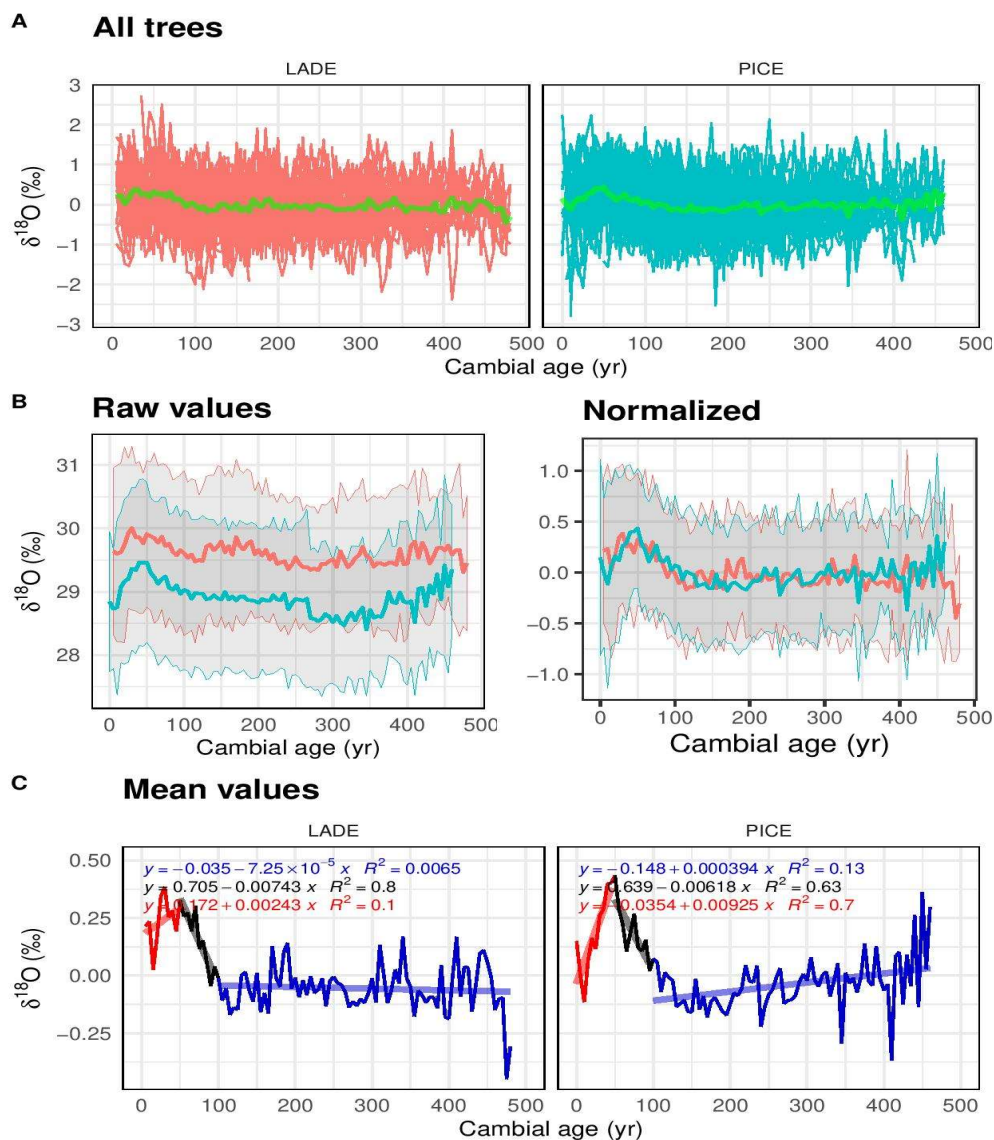
B sample number



435 **Figure 2. Cambial age and replication: A, graph of temporal distribution of the all trees and their cambial age. On the X axis the calendar age of the time series is displayed, that goes back to 9,000 yr, on the Y axis the cambial age. Each line represents a tree, in red the larch and in green the cembran pine. B, graph of the replication along the cambial age, the dotted line represents the threshold of 10 that we have considered for the analysis.**



440 **Figure 3.** Analysis of $\delta^{13}\text{C}$ data: Panel A, normalized $\delta^{13}\text{C}$ values of all larch (LADE, red) and cembran pine (PICE, green) trees, green line corresponds to the mean. Panel B, raw (left) and normalized (right) mean value with corresponding ± 1 standard deviation (grey area), of larch (red) and cembran pine (cyan). Panel C, plots of the mean values with linear approximations for periods 1-100 yr and >100 yr.

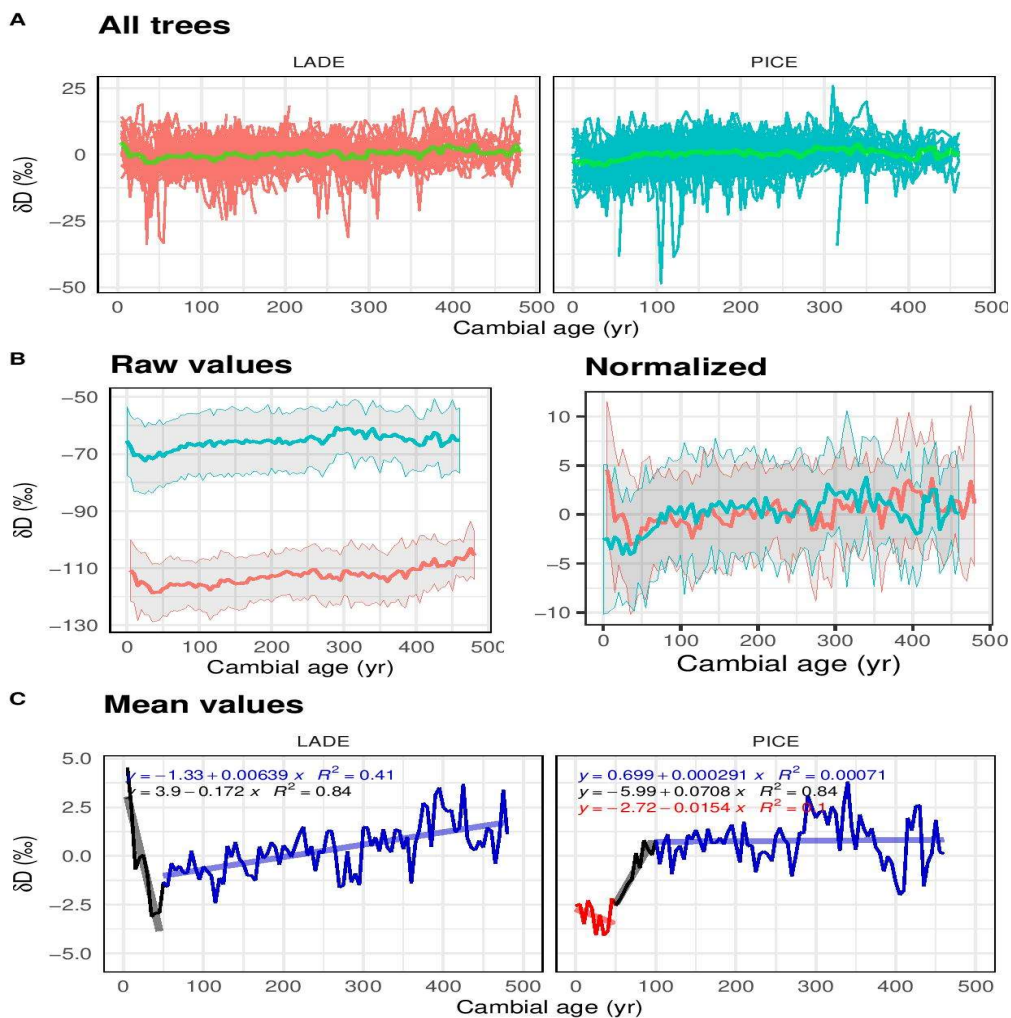


445

Figure 4. Analysis of $\delta^{18}\text{O}$ data: Panel A, normalized $\delta^{18}\text{O}$ values of all larch (LADE, red) and cebran pine (PICE, green) trees, green line corresponds to the mean. Panel B, raw (left) and normalized (right) mean value with corresponding ± 1 standard deviation (grey area), of larch (red) and cebran pine (cyan). Panel C, plots of the mean values with linear approximations for periods 1-50 yr, to 51-100 yr and >100 yr.



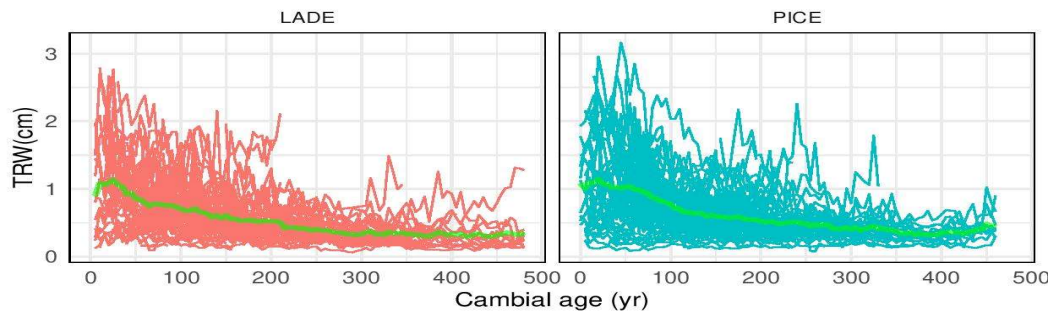
450



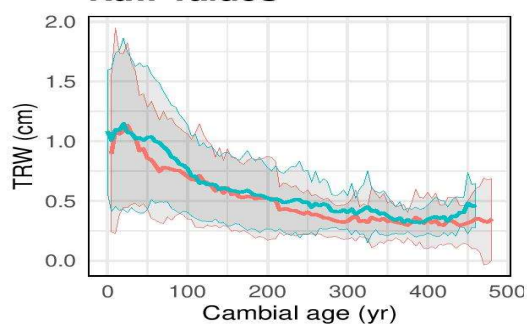
455 **Figure 5.** Analysis of δD data: Panel A, normalized δD values of all larch (LADE, red) and cembran pine (PICE, green) trees, green line corresponds to the mean. Panel B, raw (left) and normalized (right) mean value with corresponding ± 1 standard deviation (grey area), of larch (red) and cembran pine (cyan). Panel C, plots of the mean values with linear approximations for periods 1-50 yr, to 51-100 yr and >100



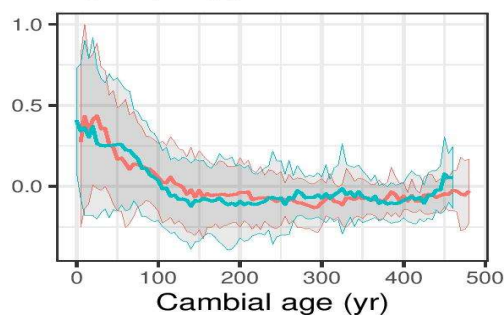
A All trees



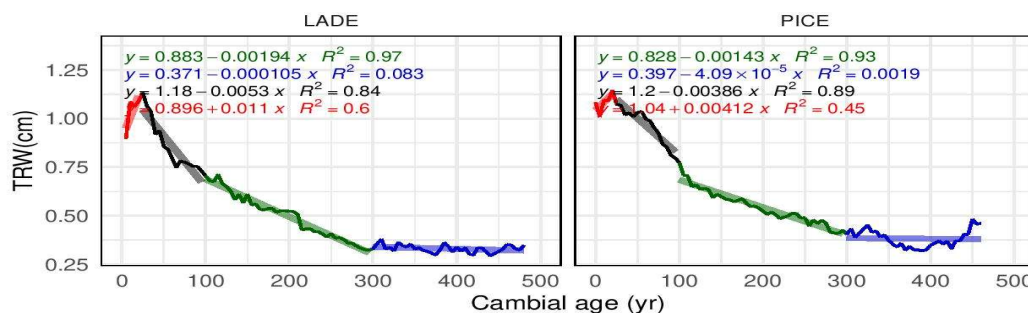
B Raw values



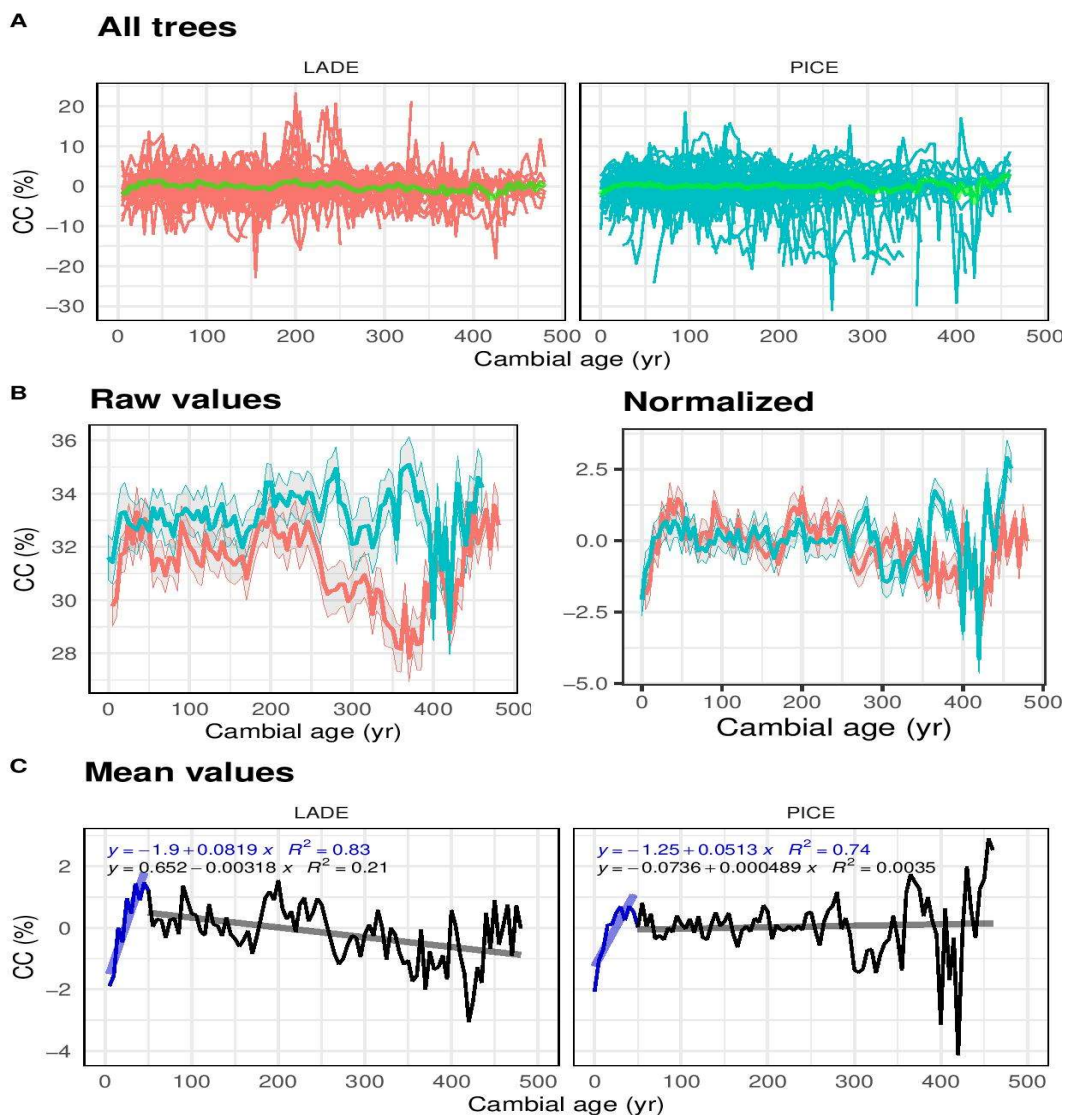
Normalized



C Mean values



460 **Figure 6.** Analysis of Tree Ring Width (TRW) data: Panel A, raw TRW values of all larch (LADE, red) and cembran pine (PICE, green) trees, green line corresponds to the mean. Panel B, raw (left) and normalized (right) mean value with corresponding ± 1 standard deviation (grey area), of larch (red) and cembran pine (cyan). Panel C, plots of the mean values with linear approximations for periods 1-50 yr, to 50-100 yr, to 101-300 yr and >300 yr..



465 **Figure 7.** Analysis of Cellulose Content (CC) data: Panel A, raw value of all larch (LADE, red) and cembra pine (PICE, green) trees, green line corresponds to the mean. Panel B, raw (left) and normalized (right) mean value with corresponding ± 1 standard deviation (grey area), of larch (red) and cembra pine (cyan). Panel C, plots of the mean values with linear approximations for periods 1-50 yr and >50 yr.